

Superimposition of Pulses to Steady Arc Discharge in Toroidal Divertor Simulator

Shin KAJITA, Tetsuya UCHIYAMA¹⁾ and Noriyasu OHNO¹⁾

EcoTopia Science Institute, Nagoya University, Nagoya 464-8603, Japan

¹⁾*Graduate School of Engineering, Nagoya University, Nagoya 464-8603, Japan*

(Received 4 March 2012 / Accepted 31 May 2012)

A pulsed discharge was superimposed to a steady state arc discharge in the toroidal divertor simulator NAGDIS-T. The dynamic response of the plasma was observed with an electrostatic probe and fast framing camera. In the first loop plasma, which is close to the plasma source, the density becomes higher in response to the pulsed discharge, and the emission from the plasma significantly increases. On the other hand, in the second loop plasma, where a recombining plasma is formed, the emission from the plasma disappears in response to the pulse. Just after the pulsed discharge, plasma instabilities were formed and they were propagated from the upstream to downstream at the velocity of ~ 10 km/s. After the series of pulsed plasma experiments, arc trails were recorded around the cathode area. On a molybdenum cover of the cathode, unipolar arcing was initiated on the surface. It is likely that the pulsed discharge leads to instabilities and initiate the unipolar arcing consequently.

© 2012 The Japan Society of Plasma Science and Nuclear Fusion Research

Keywords: NAGDIS-T, pulse superimposition, unipolar arcing

DOI: 10.1585/pfr.7.1405100

1. Introduction

In nuclear fusion research, one of the major concerns is the material erosion and damages accompanied with transient events called edge localized modes (ELMs) and disruption [1, 2]. In addition to a steady heat load of ~ 10 MWm⁻², the heat load to divertor plate in the mitigated type-I ELMs of ITER is likely to reach ~ 0.5 MJm⁻² with the time period of less than 1 ms. The material damage and erosion may deteriorate the core plasma performance and shorten the lifetime of the plasma facing material.

To demonstrate the transient heat load, experiments using pulsed laser [3, 4], plasma gun [2, 5], and electron beam [6] have been conducted. Formation of various types of cracks and droplets were observed, and moreover, initiation of arcing in response to the transients was identified. Furthermore, superimposition of pulses to steady state discharge has been demonstrated in linear divertor simulators. They were important mainly from the following two points: the influence of the pulses to the steady state plasma and the impact of pulses to the materials damaged by the steady state plasma irradiation. For the former points, the interaction between recombining detached plasmas [7] and pulses will be important in particular. In NAGDIS-II [8], in which a heated LaB₆ was used to produce plasmas, a plasma heat pulse was produced by modulating the discharge current, and the dynamic response of detached recombining plasmas to plasma heat pulse was investigated. Recently, in pilot-PSI device, transients

were generated in addition to the steady state plasma by transiently increasing the input power using a capacitor bank [9]. In pilot-PSI, a cascaded arc plasma source was used for the discharge. Investigations in the interaction between the transients and materials exposed to the steady state plasma have been started in pilot-PSI.

In this study, pulsed power is additionally superimposed to an arc discharge in the toroidal shaped divertor simulator NAGDIS (Nagoya Divertor Simulator)-T. There is an advantage in NAGDIS-T that experiments related with the issue that cannot be dealt in linear divertor simulators can be conducted. As changing the magnetic configuration, the length of the magnetic field lines can be controlled and the curvature and grad *B* effects may be observed. In particular, since the length of the magnetic field can be longer than that in the linear devices with a similar size, the low temperature recombining plasma can be easily formed in NAGDIS-T [10]. The dynamic response of a detached plasma to the additional pulse is observed with a fast framing camera and electrostatic probe. After the series of experiments, tracks of arcing are found on the surface of cathode material and the cover of the cathode which is at the floating potential. The direction of arc spot motion and jumping feature of arc spot are discussed. In Sec. 2, the experimental setup and the basic properties of the pulsed plasma are shown. The experimental results and discussion are provided in Sec. 3. Conclusions are given in Sec. 4.

author's e-mail: kajita.shin@nagoya-u.jp

2. Experimental Setup

Figure 1 (a) shows a schematic of top view of the experimental device, the divertor simulator NAGDIS-T [10], which is a toroidal configuration DC (direct current) arc discharge plasma device. A directly heated zigzag shaped LaB₆ was used for the cathode. An RF plasma source had been used for the plasma production in NAGDIS-T [11]; recently, the directly heated cathode has been used to produce high density plasma more efficiently. The electron density in NAGDIS-T is in the range of 10^{18} - $2 \times 10^{19} \text{ m}^{-3}$, and the temperature is typically less than 5 eV. Helium gas was used for the discharge gas in the present study, and the pressure was typically 20 mTorr. The toroidal and vertical magnetic coils produce magnetic fields, of which the strengths are typically 70 mT in toroidal direction and 3 mT in vertical direction. By changing the incident angle of the magnetic field line to the target plate, the connection length can be controlled from 40 to 300 m. As changing the incident angle by changing the vertical and horizontal magnetic field strengths, the number of loop is also changed. In this study, the number of loop was two. Since the plasma source is equipped in the upper side of the chamber, the plasma produced with the plasma source flowed downward as rotating in toroidal direction. The upper and lower loops are called first loop and second loop, respectively, in this paper.

Figure 1 (b) shows a diagram of the electric circuit used in the experiments. In addition to a DC power supply (Matsusada Precision Inc., 300 V, 50 A), a pulse power

supply (Aichi Electric Co., 5 kV, 200 A) was connected in parallel to the DC power supply, as shown in Fig. 1 (b). Diodes were used in order not to flow the current from one power supply to the other. Dynamic response of the plasma was observed with a fast framing camera (Photoron, Inc.: FASTCAM-MAX120) at the section nine, as shown in Fig. 1 (a). Electrostatic probes were equipped at the sections eight and twelve. The probe at the section eight measures the plasma in the first loop, while the probe at the section twelve measures the plasma in the second loop. The distance between the probes along the magnetic field line was ~ 3.3 m. For visible spectroscopy, a Czerny-Turner spectrometer (1800 grooves/mm grating, 0.75-m focal length) with a 1024×256 -pixels charge coupled device (CCD) detector was used. A lens and an optical fiber were used to collect the light emission from the plasma.

Figures 2 (a), (b), and (c) show the temporal evolutions of discharge voltage, current, and power, respectively, at the capacitor voltage of 400 V. The duration of the pulse was approximately 0.25-0.3 ms. The discharge voltage and current, which were lower than 100 V and 10 A, respectively, before the pulse, jumped in response to the superimposition of the pulse. The voltage was swiftly returned to the initial value, but the current was slightly higher even after the pulse. This is probably because the cathode surface was heated by the pulsed heat load and the electron emission was enhanced for some time, typically several ms. Figure 3 shows the peak discharge power as a function of the capacitor voltage. The discharge power increased

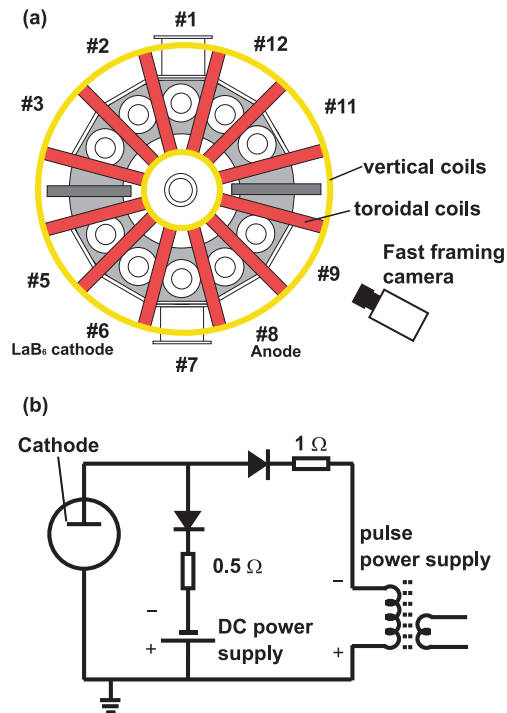


Fig. 1 Schematics of the experimental setup. (a) is a top view of NAGDIS-T and (b) is an electric circuit for the discharge.

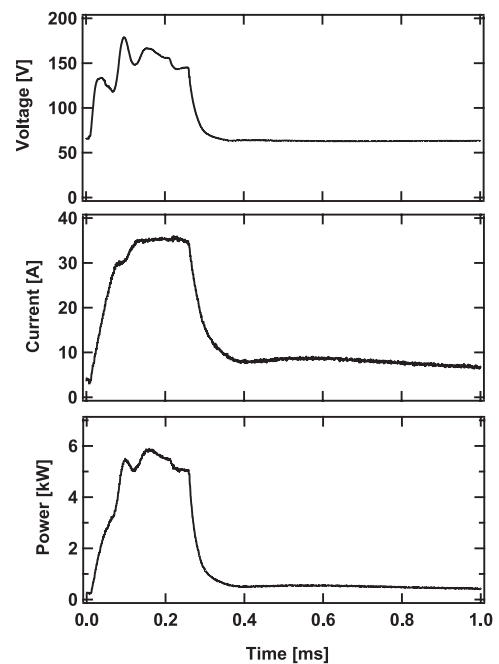


Fig. 2 Temporal evolution of typical (a) discharge voltage, (b) discharge current, and (c) discharge power in response to the pulse. The capacitor voltage was 400 V.

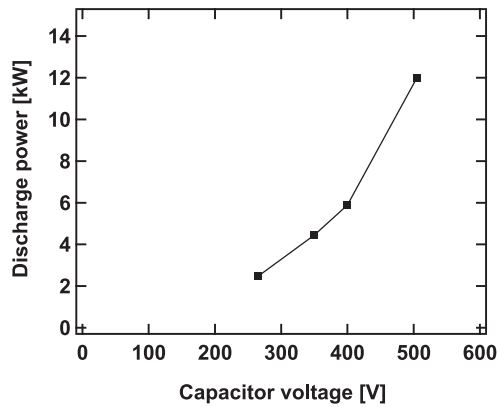


Fig. 3 The peak discharge power plotted as a function of the capacitor voltage.

with the capacitor voltage, and it reached 12 kW when the capacitor voltage was 525 V. It is expected that the power increases with the capacitor voltage further when the voltage is higher than 525 V. However, because the voltage limit of the present electric circuit was 600 V, the power could not be increased more, though the maximum voltage and current of the pulse power supply were higher.

3. Results and Discussion

3.1 Dynamic response of plasma

Figure 4 shows a picture of the plasma observed from the viewing port of section nine. Helium gas was used for the discharge gas, and the neutral pressure was 17.7 mTorr. The discharge voltage and current were 205 V and 1 A, respectively. In a deuterium plasma, the size of the plasma was expanded broadly when the plasma was in the recombining phase [10]. In the same manner, the helium plasma in the second loop expanded broadly in vertical direction when the plasma was in the recombining phase. Even though the discharge current was low, the recombining plasma was formed, because the temperature gradually decreases along with the magnetic field line and the rate coefficient of the electron ion recombination processes significantly increases as decreasing the temperature. In Fig. 4(b), spectra from the second loop are shown. Emissions from highly excited helium atoms up to $n = 13$, where n is the principal quantum number, are seen in the 2^3P-n^3D system. Thus, it can be said that recombining plasma is formed in the second loop. Probably, the recombining plasma was formed from the middle of the first loop.

Figures 5(a) and (b) show the temporal evolution of discharge power and floating potentials in the first and second loops, respectively. These are the typical response of the floating potentials. In the first loop, the floating potential increased during the pulse. The potential dropped after the pulse at ~ 0.3 ms, but again increased and had a peak around 1 ms, and then, gradually recovered to the initial values. There existed a difference in the initial phase

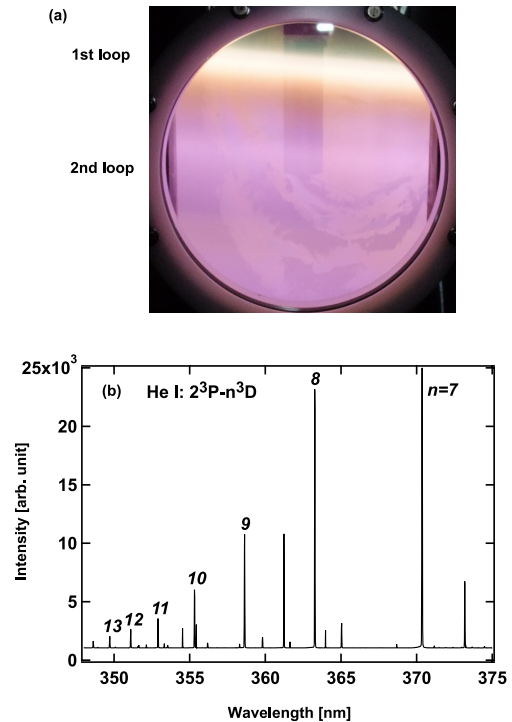


Fig. 4 (a) A picture of the emission of plasma from the first and second loops. (b) A typical spectrum from the second loop where recombining plasma was formed.

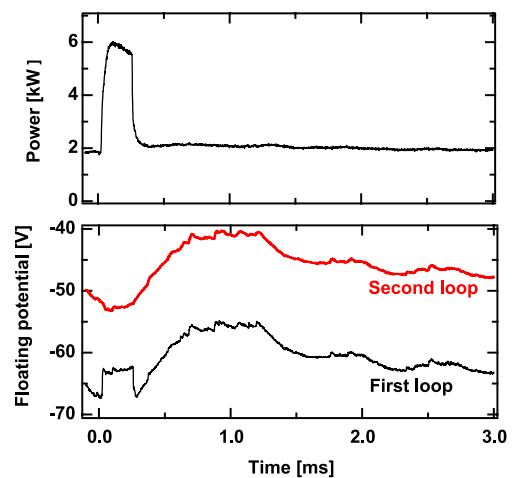


Fig. 5 The temporal evolutions of (a) discharge power and (b) floating potential in the first and second loops.

until 0.25 ms between the first and second loops. In the second loop, the floating potential decreased during the pulse, while in the first loop it increased in the same period of time. Considering the fact that the floating potential reflects the temperature of the plasma, the difference in the response of the floating potential indicated that the temperature increased in the second loop. After the pulse, i.e. > 0.5 ms, the floating potentials in the first and second loops behaved in a same manner. At present, it is not

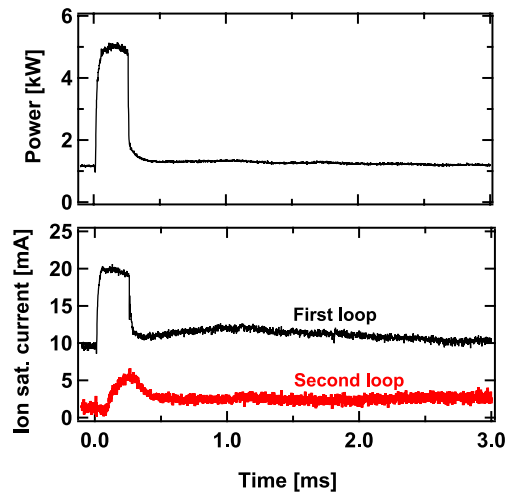


Fig. 6 The temporal evolutions of (a) discharge power and (b) ion saturation currents in the first and second loops.

clear whether these evolutions reflect the evolution of the temperature or the space potential. It would be much better if we could get the temperature from the probe current voltage characteristics. However, in the present situation, in addition to a difficulty to get the current voltage characteristics in a pulsed discharge, the probe characteristics becomes anomalous, since the plasma in the second loop is a recombining plasma [12], and the electrostatic probe cannot work properly. Other diagnostics is required for the further investigation.

Figures 6 (a) and (b) show the temporal evolutions of discharge power and ion saturation currents in the first and second loops, respectively. The current in the first and second loops both increased by the pulse superimposition. The ion saturation current in the first loop increased sharply in response to the input power. On the other hand, in the second loop, the response was delayed and current increased and decreased slowly with the time response of roughly 0.1 ms.

Figures 7 (a)–(c) show the emission profile observed with the fast framing camera (a) before the pulse (−1.2 ms), (b) during the pulse (0.1 ms), and (c) after the pulse (1.0 ms). A black vertical bar seen around the center in the figures is an anode. The temporal evolution of the vertical emission profile is shown in Fig. 8 (a). During the pulse, the emission at the first loop became significantly intense and the width of emission region became wider, while at the second loop, the emission disappeared. At 1.0 ms, the intensity at the first loop was weaker than the initial intensity and the width of the emission region was thinner. In the second loop, the plasma was probably in the recombining phase before the pulse. From the fact that the floating potential in the second loop decreased as shown in Fig. 5 (b), it was likely that the electron temperature increased in response to the pulse, and, consequently, the recombining plasma disappeared. It is known that there

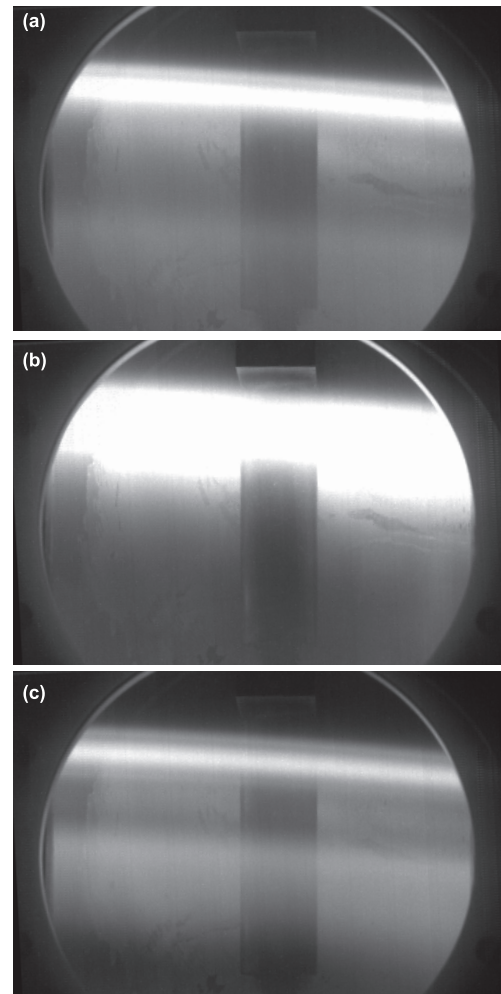


Fig. 7 The emission observed with a fast framing camera (a) before the pulse (−1.2 ms), (b) during the pulse (0.1 ms), and (c) after the pulse (1.0 ms).

existed a dark regime in between the ionizing plasma and recombining plasma [13]. From the probe measurement, it was indicated that the temperature in the second loop increased during the pulse was injected. It is thought that a slight temperature increase destroyed the recombining plasma and the recombining components of the emission disappeared.

In the second loop, the emission was recovered, but the position of the plasma was somewhat shifted to upward. As seen in Fig. 8 (a), the vertical shift of the plasma of the second loop occurred several times after the pulse. Figure 8 (b) shows the temporal evolution of the emission from the first and second loop. Before the vertical shift of the second loop took place, the intensity increased in the first loop. The intensity in the second loop increased when the vertical shift occurred. Thus, it is supposed that disturbances occurred in the plasma source region propagated to the downstream. The time difference between the increases in intensity in the first loop and second loops was approximately 0.2 ms. Since the distance between the first

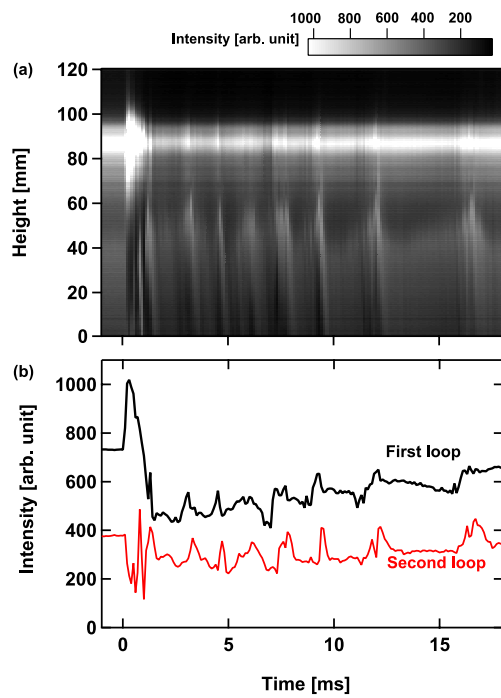


Fig. 8 (a) The temporal evolution of the vertical emission profile. (b) The time evolutions of first and second loops.

and second loops was 2.2 m, the propagation velocity was estimated to be ~ 10 km/s, which is close to the sound velocity in the ionizing plasma.

3.2 Initiation of unipolar arcing

After the series of experiments, many arc trails were found on the cathode area. Figures 9 (a) and (b) show a picture of a cover plate of the cathode and a picture of the cathode plate, respectively, after the experiments. Since such trails have not been observed in the NAGDIS-T before this series of experiments, it is highly likely that the arcing was initiated in response to the superimposition of the pulses. It is interesting to note that the arcing corresponds to unipolar arcing, because the cover plate of the cathode was at the floating potential during the experiments. In unipolar arcing, the electric emission from the cathode spot is compensated by total current flow to the surface from the surrounding plasma and local current produced with arcing [14, 15]. Although the outside of the molybdenum cover was not directly exposed to the helium plasma, the inside of the cover should be attached to the plasma. Therefore, the current to the cover from the plasma in the cathode side might have supported to sustain the arcing, which was initiated outside the cover.

In the trails, many treeing features can be seen, and they globally extended to some direction. It has been revealed recently that the arc trail has a self-affine fractality [16] in the existence of weak magnetic field, typically, say 0.05-0.5 T [17]. Although the detailed fractal analysis was not conducted for the trail shown in Fig. 9 (a), since

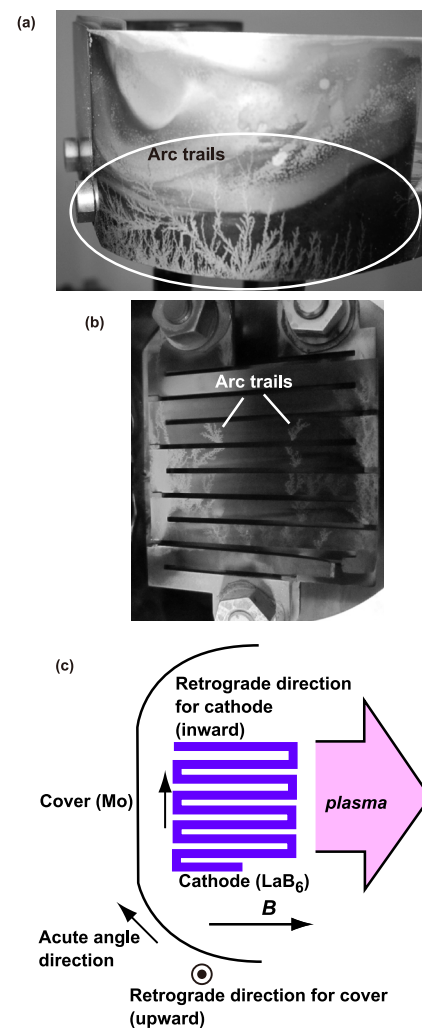


Fig. 9 (a) A pictures of the cover plate of the cathode, (b) picture of the cathode (LaB_6) plate after the series of pulse discharge experiments, and (c) a schematic of the arc spot motion.

the magnetic field strength was approximately 70 mT, the local fractality might be close to two, say around 1.8. A schematic of the direction of the arc spot with cathode and cover is shown in Fig. 9 (c). The global direction is determined by the configuration between the magnetic field and surface. When there is no cross surface magnetic field, the arc spot moves retrograde ($-j \times B$) direction. Since the direction of the current is surface normal directed to the surface, the retrograde direction corresponds to inward direction for the cathode, as seen in Fig. 9 (b). On the other hand, for the cover, the retrograde direction is upward direction. In addition, on the cover, because it has a round shape on the corner, cross field components arises there. Some trail shown in Fig. 9 (a) directed to upper left. The left direction arose by the acute angle rule [18] for cross surface component.

Another interesting point here can be seen in the trail observed in Fig. 9 (b). The cathode had a zigzag shape,

and there existed a gap of several mm in between each structure. Interestingly, it seems that the arc trail jumped from a structure to structure and run transverse direction in Fig. 9 (b). Usually, arcing is thought to be terminated when such a groove existed. In the unipolar arc trail observed in LHD, the arc spot could not jump a narrow scratch on the nanostructured tungsten [19]. In vacuum arc, sometimes the jumping phenomena was observed [20]. In ref. [20], the arc voltage jump was observed before the jump; in the present situation, it was difficult to increase the arcing voltage, because the voltage was determined between the plasma and cathode. It is likely that the surrounding high density plasma and the high temperature electron emitting cathode supported the jumping of arcing. It was thought that segmentation of the plate suppressed the continuation of arcing in the existence of magnetic field, because the arc spots usually could not cross segments. However, the result indicates that the arc may jump between segments when some conditions are satisfied. At present, the necessary conditions are not clear, and it is of interest to investigate further about this jumping phenomenon of arcing.

4. Conclusion

A pulsed power was superimposed to a steady state arc discharge in the toroidal divertor simulator NAGDIS-T. The pulse duration was approximately 0.25-0.3 ms and the input power was increased to 12 kW. From the floating potential measurement using electrostatic probes in the first and second loops, which correspond to upstream and downstream, respectively, the potential increased in the first loop, while the potential decreased in the second loop during the pulse. The result indicated that the temperature in the second loop increased significantly in response to the pulse superimposition. The ion saturation current increased in both the first and second loops. From the observation of the dynamic plasma response using a fast framing camera, it was found that the emission in the first loop increased significantly; the intensity in the second loop decreased during the pulse. The observation indicated that the recombining plasma formed in the second loop was destroyed by the pulse injection, and consequently, the temperature increased and the emission intensity decreased because there is a dark regime in between recombining and ionizing regimes. After the pulsed discharge, plasma instabilities produced in the plasma source region propagated from to the second loop. The plasma in the second loop shifted vertically in response to the instabilities and the propagation velocity obtained from the propagation of the emission was ~ 10 km/s.

After the series of pulsed plasma experiments, arc trails were recorded on the cathode and cover of the cathode. The spots moved in the retrograde direction and acute angle direction by the influence of the magnetic field. Since the cover plate was electrically disconnected, the

arcing on the cover corresponded to the unipolar arcing. Interestingly, on the cathode surface, the jumping phenomena of arc spots were observed. It is highly likely that the pulse superimposition triggered the arcing and unipolar arcing.

Acknowledgements

Authors thank excellent technical support by Mr. M. Takagi. This work is supported in part by a Grant-in-Aid for Young Scientists (A) 23686133 and Grant-in-Aid for Scientific Research (A) 22246120 from Japan Society for the Promotion of Science (JSPS).

- [1] G. Federici, A. Loarte and G. Strohmayer, *Plasma Phys. Control. Fusion* **45**, 1523 (2003).
- [2] I. Garkusha, A. Bandura, O. Byrka, V. Chebotarev, I. Landman, V. Makhraj, A. Marchenko, D. Solyakov, V. Tereshin, S. Trubchaninov and A. Tsarenko, *J. Nucl. Mater.* **337-339**, 707 (2005).
- [3] S. Kajita, S. Takamura, N. Ohno, D. Nishijima, H. Iwakiri and N. Yoshida, *Nucl. Fusion* **47**, 1358 (2007).
- [4] S. Kajita, S. Takamura and N. Ohno, *Nucl. Fusion* **49**, 032002 (2009).
- [5] Y. Kikuchi, D. Nishijima, M. Nakatsuka, K. Ando, T. Higashi, Y. Ueno, M. Ishihara, K. Shoda, M. Nagata, T. Kawai, Y. Ueda, N. Fukumoto and R. Doerner, *J. Nucl. Mater.* **415**, S55 (2011).
- [6] T. Hirai, G. Pintsuk, J. Linke and M. Batilliot, *J. Nucl. Mater.* **390-391**, 751 (2009).
- [7] P. Stangeby, *The Plasma Boundary of Manegic Fusion Devices* (IoP Publishing, Bristol and Philadelphia, 2000).
- [8] N. Ohno, M. Tanaka, N. Ezumi, D. Nishijima, S. Takamura, S.I. Krasheninnikov, A.Y. Pigarov and J. Park, *Phys. Plasmas* **6**, 2486 (1999).
- [9] G.D. Temmerman, J. Zielinski, S. van Diepen, L. Marot and M. Price, *Nucl. Fusion* **51**, 073008 (2011).
- [10] K. Yada, N. Matsui, N. Ohno, S. Kajita, S. Takamura and M. Takagi, *J. Nucl. Mater.* **390-391**, 290 (2009).
- [11] M. Nagase, H. Masuda, N. Ohno, S. Takamura and M. Takagi, *J. Nucl. Mater.* **363-365**, 611 (2007).
- [12] N. Ohno, N. Tanaka, N. Ezumi, D. Nishijima and S. Takamura, *Contrib. Plasma Phys.* **41**, 473 (2001).
- [13] F. Scotti, S. Kado, A. Okamoto, T. Shikama and S. Tanaka, *Plasma Fusion Res.* **1**, 054 (2006).
- [14] A. Robson and P. Thonemann, *Proc. Phys. Soc.* **73**, 508 (1959).
- [15] F. Schwirzke, *J. Nucl. Mater.* **128-129**, 609 (1984).
- [16] S. Kajita, N. Ohno, Y. Tsuji, H. Tanaka and S. Takamura, *J. Phys. Soc. Jpn.* **79**, 054501 (2010).
- [17] S. Kajita, S. Takamura and N. Ohno, *Plasma Phys. Control. Fusion* **53**, 074002 (2011).
- [18] A. Anders, *Cathodic Arcs: From Fractal Spots to Energetic Condensation* (Springer, New York 2008).
- [19] M. Tokitani, S. Kajita, S. Masuzaki, Y. Hirahata, N. Ohno, T. Tanabe and L.E. Group, *Nucl. Fusion* **51**, 102001 (2011).
- [20] S. Barengolts, G. Mesyats and D. Leonidovich Shmelev, *IEEE Trans. Plasma Sci.* **31**, 809 (2003).